Overexpression of *NDRG1* inhibits cell migration of breast cancer cells via reactive oxygen species during reoxygenation

Liang-Chuan Lai[1], Kuo-Chih Chen[1], Yi-Yu Su[1], Mong-Hsun Tsai[2], Yuh-Pyng Sher[4], Tzu-Pin Lu[3], and Eric Y. Chuang[3†]

[1]Graduate Institute of Physiology, [2]Institute of Biotechnology, [3]Graduate Institute of Biomedical Electronics and Bioinformatics, National Taiwan University, Taipei, Taiwan; [4]Graduate Institute of Clinical Medical Science, China Medical University, Taichung, Taiwan.

[†]Address correspondence to: Eric Y. Chuang, Department of Electrical Engineering, Graduate Institute of Biomedical Electronics and Bioinformatics, National Taiwan University, Taipei 106, Taiwan, Phone: 886-2-3366-3660, Fax: 886-2-3366-3682, E-mail: chuangey@ntu.edu.tw

Running Title: overexpression of *NDRG1* inhibits cancer migration

The author(s) indicated no potential conflicts of interest.

Abstract

One characteristic of tumor microenvironment is oxygen fluctuation, which results from hyper-proliferation and abnormal metabolism of tumor cells as well as disorganized neo-vasculature. Reoxygenation in tumor microenvironment can induce oxidative stress, which further leads to DNA damage and genomic instability. Although multiple cellular responses are activated in order to survive under this microenvironment, little is known about the dynamic response upon reoxygenation. Therefore, in order to investigate the genomic response of tumor adaptation to reoxygenation, a breast cancer cell MCF-7 was cultured under 0.5% of hypoxia for 24h followed by 24h of reoxygenation in normoxia. Cells were harvested respectively at 0, 1, 4, 8, 12, and 24h during reoxygenation. The genomic profiling of MCF-7 upon reoxygenation was examined using Illumina Human-6 v3 BeadChips. We identified 127 differentially expressed genes with 53.1% of them up-regulated and 46.9% down-regulated upon reoxygenation. Pathway analysis revealed that HIF-1-alpha transcription factor network was most significantly (P=2.02x10^{-3}) enriched in these differentially expressed genes. Among these genes, selected genes of interest were validated by quantitative real-time PCR and *NDRG1* was further investigated its function by genetic approaches. Upon reoxygenation, overexpression of *NDRG1* inhibited cell migration, and this inhibition could be relieved by reactive oxygen species scavengers. Our results revealed dynamic genomic profiling of MCF-7 upon reoxygenation, and proofed that *NDRG1* were involved in tumor adaptation to reoxygenation.

Keywords: reoxygenation, microarray, *NDRG1*, ROS, migration

Introduction

Tumor populations need overcome distinct micro-environmental barriers prior to metastasize to other organs. Invasive cancer, therefore, could be viewed as a sequence of adaptations in the phenotype to these microenvironments. The tumor microenvironment was characterized by nutrient deprivation, low pH, and hypoxia (Williams et al 2001). These changes were linked to perfusion deficits in solid tumors, which came from rapid tumor growth and profoundly disorganized vasculature (Vaupel et al 1989). These suggested that the tumor microenvironment was a unique setting for tumor progression, which required genetic and adaptive changes in cancer cells for further survival and proliferation. Cell stresses induced by the microenvironment, especially hypoxia (Bristow and Hill 2008, Corn and El-Deiry 2007) and reoxygenation (Prabhakar 2001, Welbourn et al 1991), might cause these genetic and adaptive changes.

Regions of hypoxia were a common feature in solid tumors. Oxygen became limiting because of the imbalance between O_2 delivery and consumption (Gulledge and Dewhirst 1996). The deficiencies in O_2 supply were attributed to insufficient vasculature and the depletion in successive cell layers distal to the vessel lumen; the increase of O_2 consumption was due to the high metabolic rate of tumor cells. Many studies have been reported that hypoxic tumors were more resistant to therapy, were more malignant, and had a worse prognosis (Fyles et al 2006, Magagnin et al 2006, Nordsmark et al 1996, Nordsmark et al 2005, Nordsmark et al 2006). And this phenomenon has been demonstrated in many tumor types (Brown and Wilson 2004, Vaupel et al 2004).

Moreover, the oxygen concentration within a hypoxic region was highly variable. Since tumor vasculature was highly inefficient and unstable, periods of red blood cell fluxed to the hypoxic regions, resulting in reperfusion or reoxygenation (Brown and Giaccia 1998). Reoxygenation not only increased oxygen supply but also induced oxidative stress to the cells. This oxidative stress could cause damage to cellular macromolecules, and lead to increased genomic instability (Karihtala and Soini 2007). If tumor cells survived after

exposure to hypoxia/reoxygenation insults, they may demonstrate increases in malignancy (Hockel et al 1996), DNA over-amplification (Rofstad et al 1996), drug resistance (Sanna and Rofstad 1994), and metastatic potential (Young et al 1988). Cellular adaptation to hypoxia was well documented; nevertheless, little was known about adaptive mechanisms to reoxygenation. Therefore, we used genome-wide microarrays to investigate the dynamics of gene profiling during reoxygenation in breast cancer cells MCF-7.

Our microarray results showed that *NDRG1* had the maximal response after reoxygenation. Therefore, we then focused on investigating its functional role upon reoxygenation. Human N-myc down-regulated gene 1 (*NDRG1*), composed of 394 amino acids, was highly conserved among multicellular organisms. It was expressed ubiquitously in tissues stimulated under a wide variety of stress and cell growth-regulatory conditions, such as hypoxia response (Salnikow et al 2000a, Salnikow et al 2002), DNA damage response (Kurdistani et al 1998), heavy metal response (Salnikow et al 1999, Salnikow et al 2000b, Zhou et al 1998), cellular differentiation (Guan et al 2000, Piquemal et al 1999, Taketomi et al 2003), proliferation and growth arrest (Piquemal et al 1999), neoplasia, tumor progression and metastasis (Bandyopadhyay et al 2003, Bandyopadhyay et al 2004, van Belzen et al 1997).

It was reported that *NDRG1* strongly up-regulated under hypoxic conditions. An oncogenic and tumor-promoting role of *NDRG1* has also been reported, because it was over-expressed in various human cancers, including lung, brain, skin, kidney, and breast cancers (Cangul 2004, Gomez-Casero et al 2001). Since hypoxia was prevalent in many solid tumors, its regulation was governed by hypoxia-inducible factor 1 alpha (HIF-1α) and p53-dependent pathways. But, *NDRG1* functioned as a metastatic suppressor in prostate and colon cancers (Bandyopadhyay et al 2003, Guan et al 2000). The contradictory roles of *NDRG1* in cancer remained to be clarified, although it might be explained by their multiple cellular localizations and complex regulation by diverse physiological and pathological factors. Recently, it was reported that *NDRG1* was induced and promoted cell migration

ability under intermittent hypoxia (Toffoli et al 2009). Several studies suggested that *NDRG1* associated with metastasis and induced by hypoxia, but the regulatory mechanism of *NDRG1* still remained elusive and no one described its function under reoxygenation.

In this study, we investigated the dynamic changes of gene expression upon reoxygenation using genome-wide microarrays. The differentially expressed genes upon reoxygenation were identified. Pathway analysis revealed that these genes were significantly enriched in HIF-1-alpha transcription factor network. Among these genes, *NDRG1* was further investigated its function by genetic approaches. The functional assays revealed that cell migration of breast cancer cells during reoxygenation was drove by down-regulation of *NDRG1*.

Results

Identification of genes responsive to reoxygenation

A human breast cancer cells MCF-7 were incubated under hypoxia (0.5% of O_2 concentration) for 24 h and then shifted to normoxia conditions. Cells were harvested respectively at 0 (hypoxia control), 1, 4, 8, 12 and 24 hours after reoxygenation. Each time series was independently carried out in triplicates. After extracting total RNA, the Illumina Human-6 v3 BeadChips were used to examine the dynamics of genomic profiling upon reoxygenation. Background-adjusted signals were normalized by quantile normalization algorithm. In order to identify differentially expressed genes, t-test was used to examine the expression levels of every time point after reoxygenation versus that of time zero. The reoxygenation responsive genes were selected by choosing genes whose *P*-value of three replicates at $\geqq$1 time point was < 10^{-4}. In total, we identified 127 genes whose transcript levels were significantly deviated from time 0. Among them, 53.1% of significant genes were up-regulated and 46.9% of them were down-regulated upon reoxygenation. Most of these genes (n=112) were identified only at 1 time point, 13 genes were identified at 2 time points, and only 2 genes were identified at >2 time points. Next, principle component analysis (PCA) was applied to examine the reproducibility between different replicates and whether these differentially expressed genes could be used to distinguish their reaction time. As shown in Figure 1a, different shapes denote different replicates; different colors represent different time points. The results showed that triplicates of same time point aggregated together, indicating high reproducibility of our data. Also, different time points distribute sequentially according to the exposure time under reoxygenation. The time points of 8h, 12h, and 24h were gathered closely, indicating similar expression patterns of genes at later time points. These results showed that the differentially expressed genes could be used to differentiate the reaction time of genes upon reoxygenation.

Dynamic response of gene expression profiling upon reoxygenation

To quantitatively characterize the O_2-responsive genes at each time point during acclimatization to reoxygenation, statistical analysis (Student's t-test) of each time point versus time 0 was applied for each gene. The number of genes that significantly (P<0.0001) different from the hypoxia control were plotted in Figure 1b. The numbers of O_2-responsive genes, including both up-regulated and down-regulated, at each time were 0 at 1h, 17 at 4h, 44 at 8h, 49 at 12h, and 35 at 24h. Black bars indicate the number of genes that were identified for the first time. Gray bars indicate the number of genes that have been identified at earlier time points. For example, at 12 h, 22% of genes (11/49) had been identified at 4 or 8 hours. The result showed that genetic response upon reoxygenation was between 8 and 12 h, and was then diminished at 24 h.

In order to comprehend the expression levels of these oxygen-responsive genes, their expression values of each time point were further normalized to that of time 0 and clustered using self-organizing map analysis (Figure 1c). The heatmap showed that, in general, the intensity of up- or down-regulated genes increased as cells staying longer under reoxygenation.

Pathway analysis of genes responsive to reoxygenation

In order to understand which pathways were involved in adaptation to reoxygenation, pathway analysis was done by using NCI-Nature Pathway Interaction Database (Schaefer et al 2009). Among these 127 genes, pathway analysis revealed that, as expected, the most significantly (P<0.01) enriched pathway was HIF-1-alpha transcription factor network, and the next pathway was validated targets of C-MYC transcriptional activation (Table 1). Furthermore, to investigate which pathway was activated at each time point, pathway analyses were done separately using O_2-responsive genes identified at each time point. The results showed that genes activated at 12h were mainly involved in HIF-1-alpha transcription factor network, and that genes activated at 8h were involved in validated

targets of C-MYC transcriptional activation. In addition, genes activated at 12h were also participated in ceramide signalling pathway and coregulation of androgen receptor activity (Table 1).

Identification of *NDRG1* for functional assay

In order to validate the microarray results and to select the candidate genes for functional assay, we searched top 10 genes with the maximal changes upon reoxygenation (Table 2). The steps of selecting the top 10 genes were described as follows. First of all, the expression values were normalized to time 0, and then taken log base 2. Next, the maximal absolute $\log_2$ value of each gene was identified from the 5 time points. Lastly, the O_2-responsive genes were ranked according to the maximal changes as compared to time 0. The top 10 genes with the maximal fold changes and the time point when the maximal response occurred were listed in Table 2. Also, the expression values of these genes were validated using quantitative RT-PCR. As shown in Figure 2, the RT-PCR results were very consistent with microarray results except 1 gene. Since *NDRG1* had the maximal response upon reoxygenation, we then focused our functional study on this gene.

Over-expression of NDRG1 in MCF-7

It has been reported that *NDRG1* was expressed ubiquitously under a wide variety of stress and cell growth-regulatory conditions (Ellen et al 2008, Kokame et al 1996, Kurdistani et al 1998). It is not clear whether *NDRG1* could affect the metastatic ability of tumor cells. Therefore, transwell assays were conducted to examine migration ability of MCF-7 at different O_2 concentration. As shown in Figure 3, the migration ability of MCF-7 significantly increased upon reoxygenation, while the transcript levels of *NDRG1* were significantly decreased.

Next, since *NDRG1* was down-regulated upon reoxygenation, genetic approach by

over-expressing *NDRG1* in MCF-7 was utilized to investigate its physiological function. To proof the success of over-expression, mRNA and protein expression of NDRG1 were examined by quantitative real-time PCR (Figure 4a) and Western blotting (Figure 4b). As shown in Figure 4a&b, the transcript and protein levels of NDRG1 were significantly higher than the empty vector control.

NDRG1 inhibited cell migration under reoxygenation

To investigate the functional role of *NDRG1* in cell migration, MCF-7 cells transfected with vector encoded *NDRG1* or empty vector were inoculated to transwell for cell migration assay under normoxia, hypoxia, or reoxygenation respectively (Figure 4c). Because MCF-7 was only allowed to migrate 24 h, which was less than its doubling time (72 h), cell proliferation effect was excluded. The results showed that over-expression of NDRG1 did not alter cell migration either in normoxia or hypoxia. But under reoxygenation, over-expression of NDRG1 significantly ($P < 0.001$) inhibited cell migration (Figure 4d).

Since reoxygenation induced oxidative stress by reactive oxygen species (ROS), we hypothesized that the inhibition of cell migration through *NDRG1* expression was caused by ROS. To test this hypothesis, glutathione (GSH) or N-acetyl-L-cysteine (NAC), two common ROS scavengers, were administrated respectively 2h prior to reoxygenation. The phenomenon of migration inhibition was dramatically relieved in the presence of ROS scavengers (Figure 4d). These results suggested that ROS generated by reoxygenation activates cell migration by down-regulating the transcript levels of *NDRG1*.

Discussion

Hypoxia have been intensively investigated over the past decades based on the observations that hypoxic tumors were more resistant to therapy and had a worse prognosis (Fyles et al 2006, Hockel and Vaupel 2001, Magagnin et al 2006, Nordsmark et al 1996, Nordsmark et al 2005, Nordsmark et al 2006). However, the oxygen concentration within hypoxic tumors was highly variable, because tumor vasculature was both inefficient and unstable. The hypoxic regions could become rapidly re-perfused or re-oxygenated (Brown and Giaccia 1998). Reoxygenation generating reactive oxygen species could resulted in DNA damage and cause genomic instability (Karihtala and Soini 2007). Several studies have been reported that tumor cells displayed increases in drug resistance and metastatic potential after exposed to hypoxia/reoxygenation insults (Hockel et al 1996, Sanna and Rofstad 1994). Therefore, it is necessary to consider hypoxia and reoxygenation as two parts of the same stress response as they were inevitably associated with each other. Although cellular adaptation to hypoxia was well documented, little was known about adaptive mechanisms to reoxygenation. Here, we examined the dynamics of genome-wide gene expression during reoxygenation. Genes responsive to reoxygenation and pathways that these oxygen-responsive genes were enriched were identified. Furthermore, *NDRG1* was chosen for further functional assay. The results indicated that ROS could down-regulate *NDRG1*, which promoted the migration of transformed cells upon reoxygenation.

In this study, we investigated the dynamics of gene expression during reoxygenation in MCF-7 using genome-wide microarrays, and identify biological functional pathways responsive to reoxygenation. Principle component analysis of the oxygen-responsive

genes showed high reproducibility of this study and an interesting pattern according to the exposure time under reoxygenation, indicating the progress of differentially expressed genes upon reoxygenation. According to the number of O_2-responsive genes at different time point and heat map (Figure 1b&1c), it shows that the reactive time period of genome upon reoxygenation was between 8 and 12 hours.

Furthermore, pathway analysis revealed that these O_2-responsive genes at 12h were involved in HIF-1-alpha transcription factor network, ceramide signalling pathway, and coregulation of androgen receptor activity. It is not surprising that HIF-1-alpha transcription factor network was involved in reoxygenation, because it has been reported in a similar situation, i.e. irradiation. Following radiotherapy, tumor reoxygenation lead to nuclear accumulation of HIF-1 in response to reactive oxygen (Moeller et al 2004). Genes in the HIF-1-alpha transcription factor network include *CP* (ceruloplasmin), *NDRG1*, and *SLC2A1* (solute carrier family 2 member 1, also known as *GLUT1*). *CP* encodes a metalloprotein that is involved in iron transport across the cell membrane. Mutations in this gene cause iron accumulation, and is associated with diabetes and neurologic abnormalities (Hellman and Gitlin 2002, Hochstrasser et al 2005). *SLC2A1* encodes a major glucose transporter and may be responsible for constitutive or basal glucose uptake. Its expression is increased in several tumors and promotes tumorigenesis (Amann et al 2009, Kang et al 2002, Laudanski et al 2003). In terms of the other pathways, ceramide, a bioactive lipid, has been implicated in a variety of physiological functions including apoptosis, cell growth arrest, differentiation, cell senescence, cell migration and adhesion. The gene, enriched in ceramide signaling pathway and coregulation of androgen receptor activity, was *PAWR* (PRKC apoptosis WT1 regulator protein, also known as *PAR4*). It

encodes a transcriptional repressor and functions as a pro-apoptopic protein capable of selectively inducing apoptosis in cancer cells, specifically up-regulated during apoptosis of prostate cells by activation of the Fas pro-death pathway and co-parallel inhibition of NF-kappa-B transcriptional activity (Chakraborty et al 2001). Regarding genes responsive at 8h, they were involved in validated targets of C-MYC transcriptional activation. Genes in the pathway include *HSPA4* (heat shock 70kDa protein 4), *ODC1* (ornithine decarboxylase 1), and *SLC2A1.* *ODC1* encodes the rate-limiting enzyme of the polyamine biosynthesis pathway, and its expression is increased in several tumors (Wright et al 1995, Yoshida et al 1992). The *SCL2A1*, a major glucose transporter, was persistently expressed from 8h to 12h, implying its importance in adapting to reoxygenation.

For the gene chosen for functional analysis, human N-myc down-regulated gene 1 (*NDRG1*, also known as *CAP43, DRG1,* or *PROXY-1*) was identified as the most down-regulated genes in the top 10 candidate genes. It was highly conserved among multicellular organisms, and was first recognized as a gene whose mutation was linked to a demyelinating neuropathy (Kalaydjieva et al 1996, Kurdistani et al 1998). Neuroblastoma-derived myelocytomatosis (N-Myc), as well as c-Myc, repressed *NDRG1* by a mechanism that does not directly bind to the *NDRG1* promoter but by histone deacetylase (Shimono et al 1999). It was expressed ubiquitously under a wide variety of stress and cell growth-regulatory conditions (Ellen et al 2008, Kokame et al 1996, Kurdistani et al 1998). One of the stresses was hypoxia. It was reported that *NDRG1* strongly was up-regulated under hypoxic conditions in many solid tumors. Its regulation was complex, which may be governed by hypoxia-inducible factor 1 alpha (HIF-1α)-, N-myc-, p53-dependent pathways, and other factors involved at the transcriptional and

translational levels, or through mRNA stability.

In this study, we observed that the expression of *NDRG1* had inverse correlation with degree of metastasis. This phenomenon could be interpreted as either *NDRG1* acting against metastasis processes or metastasis blocking the induction of *NDRG1*. Therefore, in order to investigate its functional role, pcDNA3.1-NDRG1 plasmid was constructed and transfected into MCF-7. The success of over-expression was verified at both mRNA level and protein level using quantitative real-time PCR and Western blotting respectively. Transwell assay was performed to analyze the effect of NDRG1 overexpression on cell mobility at different O_2 concentrations. We found that overexpression of NDRG1 in MCF-7 specifically inhibited cell migration under reoxygenation. These results implicated that NDRG1 as a metastasis suppressor, which was consistent with Maruyama's finding (Maruyama et al 2006). Although Toffoli et al reported that NDRG1 overexpression under intermittent hypoxia induced cell migration (Toffoli et al 2009), this discrepancy may be due to different type of cells and experimental setting.

In addition, in order to understand the mechanism of NDRG1 suppressing cell migration under reoxygenation, ROS scavengers, GSH and NAC, were administrated 2h prior to reoxygenation treatment. The result showed that the suppression of cell migration was rescued under reoxygenation (Fig. 4d), suggesting oxidative stress regulated cell migration through NDRG1 at the transcription level under reoxygenation.

In summary, the dynamic profiling of genes responding to reoxygenation were identified using genome-wide microarrays. Pathway analysis revealed that HIF-1-alpha transcription factor network was most significantly enriched in these differentially expressed genes. Upon reoxygenation, overexpression of NDRG1 inhibited cell migration, and this

inhibition could be relieved by reactive oxygen species scavengers. Therefore, ROS could down-regulate NDRG1, which promoted the migration of transformed cells upon reoxygenation.

Materials and methods

Cell culture

Human breast cancer cell line MCF-7 was obtained from Bioresource collection and research center (Hsiuchu, Taiwan). Human breast cancer cells MCF-7 were maintained in Dulbecco's modified Eagle's medium (DMEM, Invitrogen Life Technologies, Carlsbad, CA) containing 1.5 g/L sodium bicarbonate supplemented with 10% (v/v) fetal bovine serum (Hyclone, Gibco) and with 1% antibiotic-antimycotic solution (Invitrogen Life Technologies, Carlsbad, CA). For hypoxic cultures, cells were incubated in a hypoxia chamber (InVivo$_2$-200, Ruskinn Technology, Leeds, UK) for 24 h with a hypoxia gas mixture containing 5% CO_2, 95% N2 at 37 ^oC. The oxygen concentration in the hypoxic chamber was maintained at 0.5%. After 24 h of hypoxic growth, cells were incubated in a well humidified incubator with 5% CO_2 and 95% room air at 37 ^oC. Six samples were collected respectively at 0, 1, 4, 8, 12 and 24 hours after reoxygenation. The cells were washed with cold PBS, flash-frozen in liquid N_2, and stored at –80°C for later RNA isolation. Each experiment will be carried out in triplicate.

RNA extraction

Total RNA was extracted with TRIzol Reagent (Invitrogen, Carlsbad, CA) and was purified by RNeasy Micro cleanup kit (Qiagen, Valencia, CA) according to the manufacturer's instructions. RNA concentration and quality are determined using a NanoDrop ND-1000 spectrophotometer (NanoDrop Technologies, Wilmington, DE) and an Agilent 2100 Bioanalyzer (Agilent Technologies, Palo Alto, CA), which calculates an RNA integrity number (RIN). Total RNA (500 ng) with A260/A280 = 1.7-2.1 and RIN >7.0 are used to synthesize the first strand cDNA via reverse transcription.

Illumina human whole-genome expression beadchips

The total RNA was primed with the T7 Oligo(dT) primer and amplified by Illumina

TotalPre RNA Amplification Kit (Ambion Inc., Austin, TX) to synthesize the cDNA containing a T7 promoter sequence. Following the first strand cDNA synthesis, second strand cDNA was synthesized by converting the single-stranded cDNA into a double-stranded DNA (dsDNA) template for transcription. The reaction employed DNA polymerase and RNase H to simultaneously degrade the RNA and synthesize second strand cDNA. The double-stranded cDNA then underwent clean-up process to remove excess RNA, primers, enzymes, and salts that would inhibit in vitro transcription. Thereafter, *in vitro* transcription was conducted using the double-stranded cDNA as a template and T7 RNA polymerase to synthesize multiple copies of biotinylated cRNA. After amplification, the cRNA was mixed with an equal volume of hybridization buffer and hybridized to Illumina Human-6 v3 BeadChips (Illumina, San Diego, CA) at 58 °C for 16 hours. After hybridization, the BeadChip was washed and stained with streptavidin-Cy3 dye. The intensities of the bead's fluorescence were detected by the Illumina BeadArray Reader, and the results are analyzed using BeadStudio v3.1 software.

Data mining and statistical analysis

After scanning, the intensity data of Illumina Human-6 v3 BeadChips were analyzed by commercial software Partek® (Partek, St. Charles,MO) for mRNA expression analysis. Background-adjusted signals were normalized by quantile normalization algorithm. Quantile algorithm normalized the probe intensities based on the intensity distribution among all slides. After normalization, Principle Component Analysis (PCA), which reduces high dimensional data into 2D graph, was utilized to evaluate the similarity of the gene expression profiles. In order to identify differentially expressed genes, t-test examining the expression levels of every time point after reoxygenation versus that of time zero was utilized. Genes whose *P*-value of three replicates at at least one time point was $< 10^{-4}$ were identified and defined as O_2-responsive genes. Self-organizing map analysis and the Genesis program (Sturn et al 2002) were used to generate visual representation of

expression profiles. Furthermore, NCI-Nature Pathway Interaction Database (Schaefer et al 2009) was applied to comprehend biological functions of these differentially expressed genes.

Overexpression of *NDRG1* in MCF-7

Human *NDRG1* gene was inserted between the *EcoR I* and *BamH I* site of the eukaryotic expression vector pcDNA3.1+ (Invitrogen, Carlsbad, CA). MCF-7/NDRG1 cells were created by transfection of MCF-7 cells with pCDNA3.1+ encoding the *NDRG1* gene using lipofectamine 2000 (Invitrogen, Carlsbad, CA). MCF-7/NDRG1 cells were then selected by 200 μg/ml of Zeocine for two weeks. The mRNA expression of *NDRG1* was examined by quantitative real-time PCR, and NDRG1 protein expression was examined by Western blotting.

Quantitative real-time PCR

Total RNA was extracted using TRIzol Reagent (Invitrogen, Carlsbad, CA) according to manufacturer's instructions. Reverse transcription of total RNA was performed with High Capacity cDNA RT Kit (Applied Biosystems, Foster City, CA) using random primers and 1μg total RNA as template. The reaction mixture was incubated at 25 °C for 10 min, 37 °C for 2 h and 85 °C for 5 sec. Real time PCR was detected by SYBR Green (Sigma) and was performed using the ABI 7300 (Applied Biosystems, Foster City, CA). The reactions were performed using the following program: 40 cycles of denaturing at 95 °C for 15 s and 1 min of annealing and elongating at 60 °C. For each cDNA sample, an internal control, 18s rRNA was also measured by SYBR Green probe to ensure comparable amounts of cDNA in all wells. Relative expression of *NDRG1* compared with 18s rRNA in each sample was calculated (△Ct) and relative expression of *NDRG1* among samples were determined by calculating the difference in △Ct between samples (△△Ct). All measurements were made in triplicate (5ng of total RNA per well) and repeated at least

three times.

Western blotting

Whole cell extracts were prepared using RIPA lysis buffer supplemented with 1% Nonidet P-40 (NP-40) and protease inhibitor (Roche, Mannheim, Germany). Cell debris was collected by centrifugation at 4 °C for 20 minutes. Protein concentration was measured by the bicinchoninic acid method (BCA assay), and 20~50 μg protein was loaded on a 10 % denaturing sodium dodecyl sulfate polyacrylamide gel. After electrophoresis, protein was electrophoretically transferred to PVDF membranes for overnight at 55mA. The membranes were blocked with Tris-Buffered Saline Tween-20 (TBST) with 5 % non-fat powdered milk at room temperature for an hour. Detection of specific proteins was done by probed membranes with Primary anti-NDRG1 antibody (AbCam, Cambridge, United Kingdom) at 1:500 dilutions in TBS 0.05% Tween-20/ 5% non-fat milk for 1.5 hours at room temperature. After incubation with the horseradish peroxidase-conjugated IgG secondary antibodies (1:5000), the immunoreactivity was visualized by enhanced chemoluminescence with Luminol Reagent (Bio-Rad Laboratories, Richmond, CA, USA). β-actin (1:50000) was used as a loading control.

Cell migration assay

Migration assay were carried out using 24-well transwell migration chambers (Corning, Corning, New York, USA) with 8 μm pore size of polyethylene membranes. Cells were first starved 24h and were harvested by Accutase (PAA Laboratories, Linz, Austria). The upper chambers were inoculated with $5x10^4$ cells/well in 0.1 ml serum-free DMEM cell solution, and lower chambers were filled with 0.6 ml DMEM containing 10% FBS as chemoattractant. Cells were allowed to migrate for 24 h at 37 °C. For measuring the migrated cells, 2 μg/ml Calcein-AM (Trevigen, Gaithersburg, MD, USA)/Cell Dissociation Solution (Trevigen) was added into the lower chamber. After incubation at 37

°C for 60 min, inserts were removed and plates were read at 485nm excitation and 520 nm emission. Cell numbers were calculated by comparing the absorbance of standard curve. MCF-7 transfected with empty vector was used as the control for each experiment.

ROS scavenger treatment

ROS scavengers, Glutathione (GSH, 5mmol/L) (St. Louis, MO, USA) or *N*-acetyl-L-cysteine (NAC, 5mmol/L) (St. Louis, MO, USA), were applied in DMEM medium 2 h before reoxygenation.

Conflict of interest

The author(s) indicated no potential conflicts of interest.

Acknowledgments

This research was supported in part by grants from China Medical University, Taiwan (Grant No. 97F008-119; 99F008-308). The funders had no role in study design, data collection and analysis, decision to publish, or preparation of the manuscript. Our special thanks are also due to the technicians at National Center of Excellence for Clinical Trials and Research and the Division of Genomic Medicine, National Taiwan University for their technical assistance.

REFERENCES

Amann T, Maegdefrau U, Hartmann A, Agaimy A, Marienhagen J, Weiss TS *et al*. (2009). Glut1 expression is increased in hepatocellular carcinoma and promotes tumorigenesis. *The American journal of pathology* **174:** 1544-1552.

Bandyopadhyay S, Pai SK, Gross SC, Hirota S, Hosobe S, Miura K *et al*. (2003). The drg-1 gene suppresses tumor metastasis in prostate cancer. *Cancer Res* **63:** 1731-1736.

Bandyopadhyay S, Pai SK, Hirota S, Hosobe S, Tsukada T, Miura K *et al*. (2004). Pten up-regulates the tumor metastasis suppressor gene drg-1 in prostate and breast cancer. *Cancer Res* **64:** 7655-7660.

Bristow RG, Hill RP. (2008). Hypoxia and metabolism. Hypoxia, DNA repair and genetic instability. *Nat Rev Cancer* **8:** 180-192.

Brown JM, Giaccia AJ. (1998). The unique physiology of solid tumors: Opportunities (and problems) for cancer therapy. *Cancer Res* **58:** 1408-1416.

Brown JM, Wilson WR. (2004). Exploiting tumour hypoxia in cancer treatment. *Nat Rev Cancer* **4:** 437-447.

Cangul H. (2004). Hypoxia upregulates the expression of the ndrg1 gene leading to its overexpression in various human cancers. *BMC Genet* **5:** 27.

Chakraborty M, Qiu SG, Vasudevan KM, Rangnekar VM. (2001). Par-4 drives trafficking and activation of fas and fasl to induce prostate cancer cell apoptosis and tumor regression. *Cancer Res* **61:** 7255-7263.

Corn PG, El-Deiry WS. (2007). Microarray analysis of p53-dependent gene expression in response to hypoxia and DNA damage. *Cancer Biol Ther* **6:** 1858-1866.

Ellen TP, Ke Q, Zhang P, Costa M. (2008). Ndrg1, a growth and cancer related gene:

Regulation of gene expression and function in normal and disease states. *Carcinogenesis* **29:** 2-8.

Fyles A, Milosevic M, Pintilie M, Syed A, Levin W, Manchul L *et al*. (2006). Long-term performance of interstial fluid pressure and hypoxia as prognostic factors in cervix cancer. *Radiother Oncol* **80:** 132-137.

Gomez-Casero E, Navarro M, Rodriguez-Puebla ML, Larcher F, Paramio JM, Conti CJ *et al*. (2001). Regulation of the differentiation-related gene drg-1 during mouse skin carcinogenesis. *Mol Carcinog* **32:** 100-109.

Guan RJ, Ford HL, Fu Y, Li Y, Shaw LM, Pardee AB. (2000). Drg-1 as a differentiation-related, putative metastatic suppressor gene in human colon cancer. *Cancer Res* **60:** 749-755.

Gulledge CJ, Dewhirst MW. (1996). Tumor oxygenation: A matter of supply and demand. *Anticancer Res* **16:** 741-749.

Hellman NE, Gitlin JD. (2002). Ceruloplasmin metabolism and function. *Annu Rev Nutr* **22:** 439-458.

Hochstrasser H, Tomiuk J, Walter U, Behnke S, Spiegel J, Kruger R *et al*. (2005). Functional relevance of ceruloplasmin mutations in parkinson's disease. *FASEB J* **19:** 1851-1853.

Hockel M, Schlenger K, Aral B, Mitze M, Schaffer U, Vaupel P. (1996). Association between tumor hypoxia and malignant progression in advanced cancer of the uterine cervix. *Cancer Res* **56:** 4509-4515.

Hockel M, Vaupel P. (2001). Tumor hypoxia: Definitions and current clinical, biologic, and molecular aspects. *J Natl Cancer Inst* **93:** 266-276.

Kalaydjieva L, Hallmayer J, Chandler D, Savov A, Nikolova A, Angelicheva D *et al*. (1996). Gene mapping in gypsies identifies a novel demyelinating neuropathy on chromosome 8q24. *Nat Genet* **14:** 214-217.

Kang SS, Chun YK, Hur MH, Lee HK, Kim YJ, Hong SR *et al*. (2002). Clinical significance of glucose transporter 1 (glut1) expression in human breast carcinoma. *Jpn J Cancer Res* **93:** 1123-1128.

Karihtala P, Soini Y. (2007). Reactive oxygen species and antioxidant mechanisms in human tissues and their relation to malignancies. *APMIS* **115:** 81-103.

Kokame K, Kato H, Miyata T. (1996). Homocysteine-respondent genes in vascular endothelial cells identified by differential display analysis. Grp78/bip and novel genes. *J Biol Chem* **271:** 29659-29665.

Kurdistani SK, Arizti P, Reimer CL, Sugrue MM, Aaronson SA, Lee SW. (1998). Inhibition of tumor cell growth by rtp/rit42 and its responsiveness to p53 and DNA damage. *Cancer Res* **58:** 4439-4444.

Laudanski P, Swiatecka J, Kovalchuk O, Wolczynski S. (2003). Expression of glut1 gene in breast cancer cell lines mcf-7 and mda-mb-231. *Ginekol Pol* **74:** 782-785.

Magagnin MG, Koritzinsky M, Wouters BG. (2006). Patterns of tumor oxygenation and their influence on the cellular hypoxic response and hypoxia-directed therapies. *Drug Resist Updat* **9:** 185-197.

Maruyama Y, Ono M, Kawahara A, Yokoyama T, Basaki Y, Kage M *et al*. (2006). Tumor growth suppression in pancreatic cancer by a putative metastasis suppressor gene cap43/ndrg1/drg-1 through modulation of angiogenesis. *Cancer Res* **66:** 6233-6242.

Moeller BJ, Cao Y, Li CY, Dewhirst MW. (2004). Radiation activates hif-1 to regulate

vascular radiosensitivity in tumors: Role of reoxygenation, free radicals, and stress granules. *Cancer Cell* **5:** 429-441.

Nordsmark M, Overgaard M, Overgaard J. (1996). Pretreatment oxygenation predicts radiation response in advanced squamous cell carcinoma of the head and neck. *Radiother Oncol* **41:** 31-39.

Nordsmark M, Bentzen SM, Rudat V, Brizel D, Lartigau E, Stadler P *et al*. (2005). Prognostic value of tumor oxygenation in 397 head and neck tumors after primary radiation therapy. An international multi-center study. *Radiother Oncol* **77:** 18-24.

Nordsmark M, Loncaster J, Aquino-Parsons C, Chou SC, Gebski V, West C *et al*. (2006). The prognostic value of pimonidazole and tumour po2 in human cervix carcinomas after radiation therapy: A prospective international multi-center study. *Radiother Oncol* **80:** 123-131.

Piquemal D, Joulia D, Balaguer P, Basset A, Marti J, Commes T. (1999). Differential expression of the rtp/drg1/ndr1 gene product in proliferating and growth arrested cells. *Biochim Biophys Acta* **1450:** 364-373.

Prabhakar NR. (2001). Oxygen sensing during intermittent hypoxia: Cellular and molecular mechanisms. *J Appl Physiol* **90:** 1986-1994.

Rofstad EK, Johnsen NM, Lyng H. (1996). Hypoxia-induced tetraploidisation of a diploid human melanoma cell line in vitro. *Br J Cancer Suppl* **27:** S136-139.

Salnikow K, An WG, Melillo G, Blagosklonny MV, Costa M. (1999). Nickel-induced transformation shifts the balance between hif-1 and p53 transcription factors. *Carcinogenesis* **20:** 1819-1823.

Salnikow K, Costa M, Figg WD, Blagosklonny MV. (2000a). Hyperinducibility of

hypoxia-responsive genes without p53/p21-dependent checkpoint in aggressive prostate cancer. *Cancer Res* **60:** 5630-5634.

Salnikow K, Su W, Blagosklonny MV, Costa M. (2000b). Carcinogenic metals induce hypoxia-inducible factor-stimulated transcription by reactive oxygen species-independent mechanism. *Cancer Res* **60:** 3375-3378.

Salnikow K, Kluz T, Costa M, Piquemal D, Demidenko ZN, Xie K *et al*. (2002). The regulation of hypoxic genes by calcium involves c-jun/ap-1, which cooperates with hypoxia-inducible factor 1 in response to hypoxia. *Mol Cell Biol* **22:** 1734-1741.

Sanna K, Rofstad EK. (1994). Hypoxia-induced resistance to doxorubicin and methotrexate in human melanoma cell lines in vitro. *Int J Cancer* **58:** 258-262.

Schaefer CF, Anthony K, Krupa S, Buchoff J, Day M, Hannay T *et al*. (2009). Pid: The pathway interaction database. *Nucleic Acids Res* **37:** D674-679.

Shimono A, Okuda T, Kondoh H. (1999). N-myc-dependent repression of ndr1, a gene identified by direct subtraction of whole mouse embryo cdnas between wild type and n-myc mutant. *Mech Dev* **83:** 39-52.

Sturn A, Quackenbush J, Trajanoski Z. (2002). Genesis: Cluster analysis of microarray data. *Bioinformatics* **18:** 207-208.

Taketomi Y, Sugiki T, Saito T, Ishii S, Hisada M, Suzuki-Nishimura T *et al*. (2003). Identification of ndrg1 as an early inducible gene during in vitro maturation of cultured mast cells. *Biochem Biophys Res Commun* **306:** 339-346.

Toffoli S, Delaive E, Dieu M, Feron O, Raes M, Michiels C. (2009). Ndrg1 and crk-i/ii are regulators of endothelial cell migration under intermittent hypoxia. *Angiogenesis* **12:** 339-354.

van Belzen N, Dinjens WN, Diesveld MP, Groen NA, van der Made AC, Nozawa Y *et al*. (1997). A novel gene which is up-regulated during colon epithelial cell differentiation and down-regulated in colorectal neoplasms. *Lab Invest* **77:** 85-92.

Vaupel P, Kallinowski F, Okunieff P. (1989). Blood flow, oxygen and nutrient supply, and metabolic microenvironment of human tumors: A review. *Cancer Res* **49:** 6449-6465.

Vaupel P, Mayer A, Hockel M. (2004). Tumor hypoxia and malignant progression. *Methods Enzymol* **381:** 335-354.

Welbourn CR, Goldman G, Paterson IS, Valeri CR, Shepro D, Hechtman HB. (1991). Pathophysiology of ischaemia reperfusion injury: Central role of the neutrophil. *Br J Surg* **78:** 651-655.

Williams KJ, Cowen RL, Stratford IJ. (2001). Hypoxia and oxidative stress. Tumour hypoxia--therapeutic considerations. *Breast Cancer Res* **3:** 328-331.

Wright PS, Cooper JR, Cross-Doersen DE, Miller JA, Chmielewski PA, Wagner RL *et al*. (1995). Regulation of ornithine decarboxylase mrna levels in human breast cancer cells: Pattern of expression and involvement of core enhancer promoter element. *Cell Growth Differ* **6:** 1097-1102.

Yoshida M, Hayashi H, Taira M, Isono K. (1992). Elevated expression of the ornithine decarboxylase gene in human esophageal cancer. *Cancer Res* **52:** 6671-6675.

Young SD, Marshall RS, Hill RP. (1988). Hypoxia induces DNA overreplication and enhances metastatic potential of murine tumor cells. *Proc Natl Acad Sci U S A* **85:** 9533-9537.

Zhou D, Salnikow K, Costa M. (1998). Cap43, a novel gene specifically induced by ni2+ compounds. *Cancer Res* **58:** 2182-2189.

Table 1. Enriched pathways and their *P*-values in differentially expressed genes responsive to reoxygenation.

Enriched pathway*	Genes expressed at any time point (n=127)	Genes expressed at the following time point:				
		1 h (n=0)	4 h (n=17)	8 h (n=44)	12 h (n=49)	24 h (n=35)
HIF-1-alpha transcription factor network	2.02E-03	- #	-	-	6.27E-03	-
Validated targets of C-MYC transcriptional activation	4.19E-03	-	-	3.07E-03	-	-
Ceramide signaling pathway	-	-	-	-	3.56E-03	-
Coregulation of Androgen receptor activity	-	-	-	-	5.57E-03	-

* Pathway analysis was done by using NCI-Nature Pathway Interaction Database (Schaefer et al 2009)
# - denotes *P*-value > 0.01

Table 2. The top 10 O_2-responsive genes with maximal response after reoxygenation

Rank	Gene	Max. $\log_2$ ratio[#]	Time point with max. response (h)	Description
1	*NDRG1*	-3.76	24	N-myc downstream regulated 1
2	*KRT17*	-3.45	24	Keratin 17
3	*PFKFB4*	-3.09	8	6-phosphofructo-2-kinase / fructose-2,6-biphosphatase 4
4	*VTCN1*	-2.91	24	V-set domain containing T cell activation inhibitor 1
5	*DPYSL4*	-2.91	24	Dihydropyrimidinase-like 4
6	*TGFBI*	-2.90	24	Transforming growth factor, beta-induced, 68kda
7	*GDF15*	-2.75	8	Growth differentiation factor 15
8	*SAMD4A*	-2.23	12	Sterile alpha motif domain containing 4A
9	*BNIP3L*	-2.22	12	BCL2 / adenovirus E1B 19kda interacting protein 3-like
10	*GBE1*	-2.21	24	Glucan (1,4-alpha-), branching enzyme 1

[#] The ranking of gene expression relative to time zero was determined by the maximal absolute value of $\log_2$(ratio) in the time series. Negative value denotes down-regulation upon reoxygenation.

FIGURE LEGENDS

Figure 1. Dynamics of differentially expressed genes during acclimatization to reoxygenation. (a) Principle component analysis (PCA) of O2-responsive genes in MCF7 cells during 24h of reoxygenation after hypoxia. The axes in figure are the first two principal components (PC) which can explain most of the gene expression profiling. Three independent experiments were done at each time point. Different shapes represent different replicates; different colors represent different time points. (b) Number of O_2-responsive genes at each time point during reoxygenation. The numbers of O_2-responsive genes, including both up-regulated and down-regulated, are plotted as a function of time after the shift. Black bars indicate the number of genes that were identified for the first time; whereas gray bars indicate the number of genes that have been identified at earlier time points. (c) Relative expression profiles of the O_2-responsive genes after shifting to reoxygenation. The expression values of each time point were normalized to that of time zero. The scale bar to the left denotes 20 genes, and the color bar to the right indicates the degree of gene expression change relative to time zero.

Figure 2. Quantitative real-time PCR validation of the top 10 O_2-responsive genes with the maximal response upon reoxygenation.

Figure 3. Down-regulation of *NDRG1* correlates with increase of MCF-7 migration under reoxygenation. (a) Relative migration ability of MCF-7 at different O_2 condition. Transwell assay was used to measure MCF-7 migration. The migration ability was expressed as relative fold changes to normoxia. (b) Relative expression levels of *NDRG1* at different O_2 condition. The mRNA levels of *NDRG1* measuring by RT-PCR were first normalized by 18s rRNA, and then compared to that in normoxia. *, $P<0.01$.

Figure 4. Overexpression of NDRG1 inhibits MCF-7 migration under reoxygenation. (a) Quantitative real-time PCR analysis of *NDRG1* over-expressed in MCF-7. The mRNA levels of *NDRG1* were normalized by 18s rRNA. EV: Empty vector. (b) Western blotting of NDRG1. Protein from whole cell lysates was blotted with NDRG1 specific antibody, and β-actin was the loading control. (c) Scheme of experimental design for cell migration assay. MCF-7 was inoculated to 8.0μm transwell for cell migration assay under normoxia, hypoxia, or reoxygenation respectively. (d) Effects of *NDRG1* over-expressed in MCF-7 on cell migration under normoxia, hypoxia and reoxygenation. Cell migration percentage was normalized to respective empty control. Glutathione (GSH) (5mM) or *N*-acetyl-L-cysteine (NAC) (5mM) was added as ROS scavengers 2h prior to reoxygenation. Three independent experiments

were performed. Data presented were the mean ± SE. *$P < 0.01$.

FIGURES

Figure 1. Lai et al.

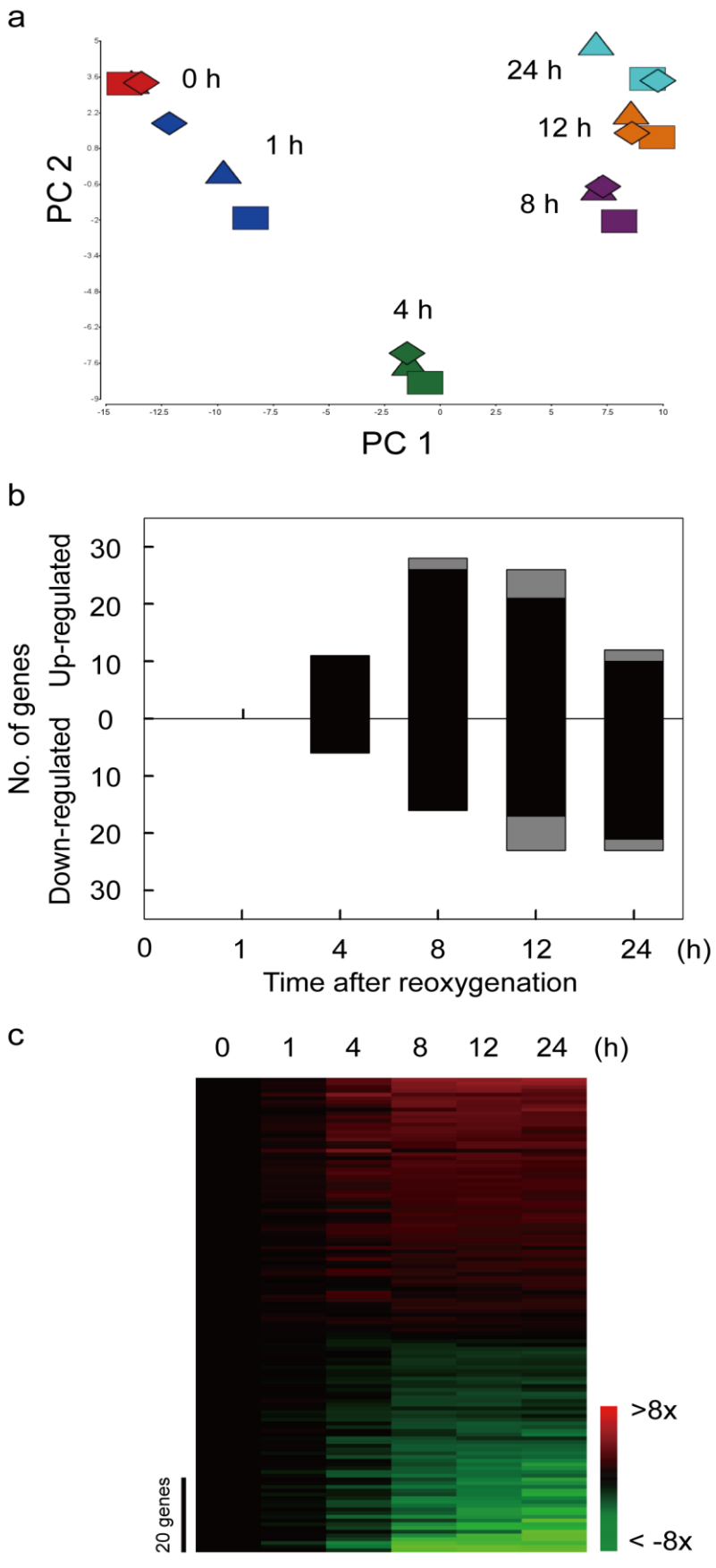

Figure 2. Lai et al.

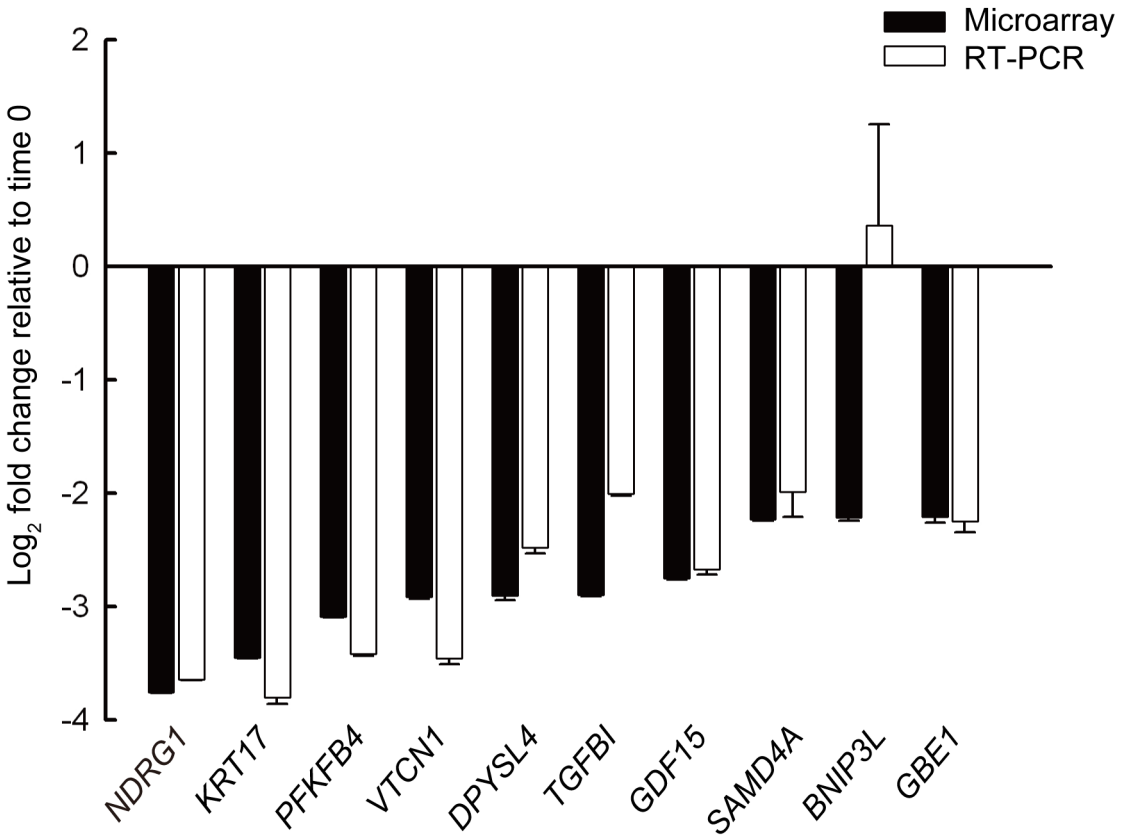

Figure 3. Lai et al.

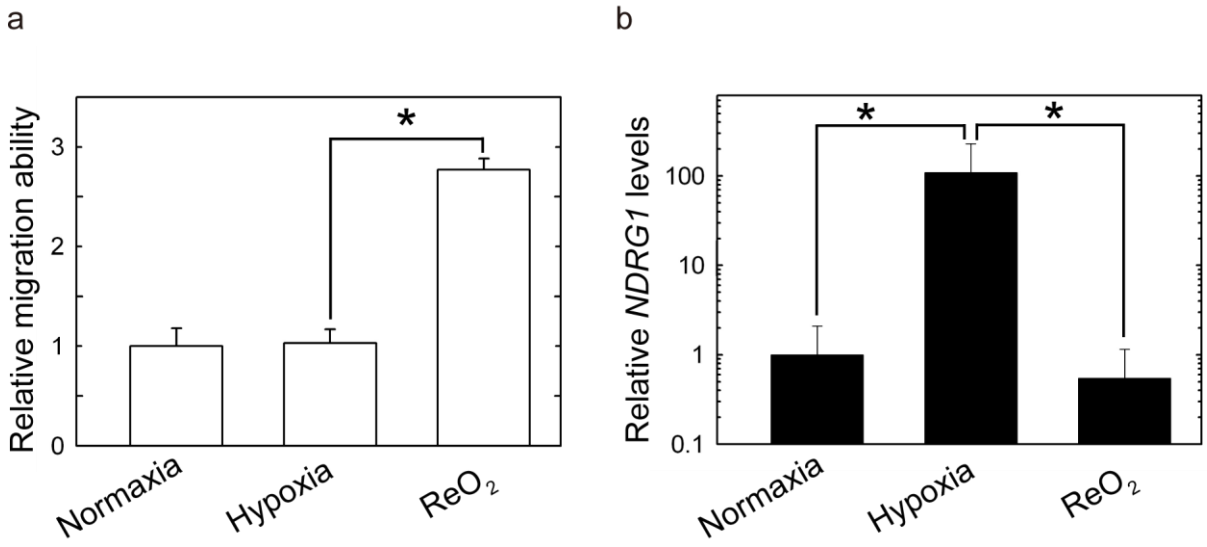

Figure 4. Lai et al.